

Design and Magnetically Analysis of Circular Flux Linear Actuator

A. Fenercioğlu

Gaziosmanpasa University, Turhal Higher Vocational School,

Turhal Meslek Yüksekokulu 60300 Turhal, Tokat, Turkey, phone: +903562757839/110, e-mail: af@gop.edu.tr

Introduction

This study deals with an actuator's design, modeling analysis, and is based on the structure of linear switched reluctance motor (LSRM). The linear structure of LSRM is divided to two pair of their magnetic flux directions being transverse or longitudinal flux. Single sided or double sided design of both is possible [1-2]. This study includes the design procedures of the double sided linear actuators with circular transverse magnetic flux, finite elements analysis (FEA) and analytical approaches.

The actuator has a simple geometrical structure and it doesn't require permanent magnet and therefore its design and production costs are low. It requires driver circuit and rotor position information. Its control system and driver design are easier than the commonly used induction motors. The developing power electronics elements and micro controllers enable usage in linear moving places with an easy and flexible control strategy [3, 4].

In the literature [2], traverse flux LSRM was examined for high power density. It has double sided quadrangular core but it has not circular structure.

The use of linear switched reluctance motors (LSRMs) for the primary propulsion of a ship elevator is proposed and investigated. A new type of LSRM is proposed with twin stators and a translator between them with no back iron in the translator [3]. It has longitudinal flux path.

A SRM drive has been investigated and recommended as an alternative actuator for vertical linear transportation

applications such as a linear elevator. A prototype home elevator with LSRMs is designed, and extensive experimental correlation is presented in literature [4].

Literature [5] presents the realization and design of a new LSRM structure. The new model has a double sided configuration and provides a high force for many applications with a low cost.

In this study, the design and 3D FEA of circular structured transverse flux linear actuator are examined.

Geometrical modeling

The actuator consists of stator and translator parts. Stator is the fixed part and called as passive stator as there is no flux supply on it. Translator is the moving part and called as active translator as it carries coils enabling movement. There are 6 pairs of translator poles which are placed with double sides. The coils on the translator enabling movement are switched with 3 phases. The movement is achieved by the addition of the 4 pairs of stator poles in the switching cycle of 3 phases to the magnetic coupling. The magnetic circuit is completed with a pair of stator pole aligned side by side longitudinally. The double poles of the stator are lined in a row longitudinally with equal distances in the movement direction and the movement distance of the actuator is extended at the desired length. Fig. 1 shows the simulated model of the actuator. The translator and stator has been designed totally yokeless [6].

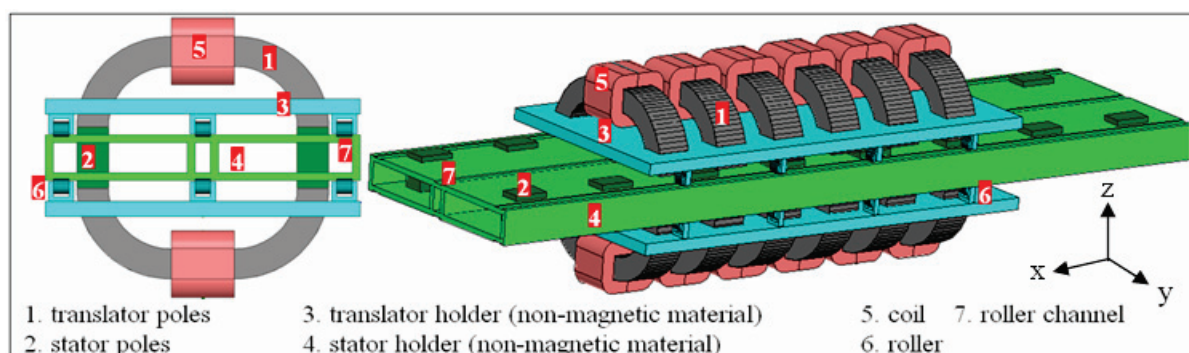


Fig. 1. Simulated model of the linear actuator

Thus each translator part of different phases has been insulated magnetically and makes the magnetic circuit independent from each other. As there is no back iron, the coils of different phases are not on a joint core. Therefore the leakage flux that may arise between phases has been minimized with this design. Besides in the event of any defect of the actuator, the defect can be repaired or replaced by removing the relevant parts instead of disassembling the whole system. It extends the movement distance by adding new stator parts. Costs have been reduced and actuator has been made lighter with yokeless design [2 - 5]. This has increased the force generated per unit mass. The sizes of the linear actuator are given in Fig. 2 and its explanations are given in Table 1.

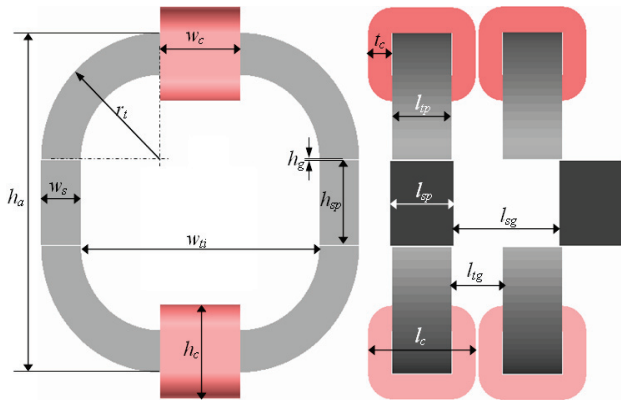


Fig. 2. Simulator model of the actuator

Table 1. The dimensional explanations of the CFLA

Symbols	Explanations	size (mm)
w_s	Width of stator	20
h_{sp}	Height of stator pole	40
l_{sp}	Length of stator pole	32
w_{ti}	Inner width of translator	120
l_{tp}	Length of translator pole	30
r_t	Outer radius of translator	40
w_c	Width of coil	40
h_c	Height of coil	44,4
t_c	Thickness of coil	12
l_c	Length of coil	54,4
l_{ig}	Length of between translator poles	30
l_{sg}	Length of between stator poles	58
h_g	Height of air gap	0,6
l_t	Length of overall translator	354,4
h_a	Height of actuator	185,6

Assumptions

The magnetic design of the linear actuator and its static magnetic analysis based upon 3 dimensional computer aided with finite elements method have been done by Maxwell 3D Software. Translator is moved in forward direction on the x axis with 5 mm steps between fully unaligned position and fully aligned position (0-45 mm) and the axial forces, inductance, magnetic flux intensity values of each position have been estimated.

The dynamic operating conditions of the actuator, control strategy and the impacts of the driver have not been taken into consideration in simulation solutions. The

magnetic core material in the motor design is taken as a whole and no lamination has been made [2, 6 and 7].

One phase consists of 4 coils and each coil is designed with one winding. Therefore the phase excitation is given as 1500 AT, 2000 AT and 2500 AT mmf. However, each coil has actually 250 windings.

Thus, it is assumed that 1500 AT (6 A x 250 turn), 2000 AT (8 A x 250 turn), 2500 AT (10 A x 250 turn) are applied to the coil to obtain the same mmf in the actual operation. The Fig. 3 shows the BH curve of the material used in the simulation. As the simulations are done with the 3 dimensional finite elements analysis, the effects of the factors that may affect the parameters have been taken into consideration like saturation, leakage flux, fringing and relative permeability [6–8].

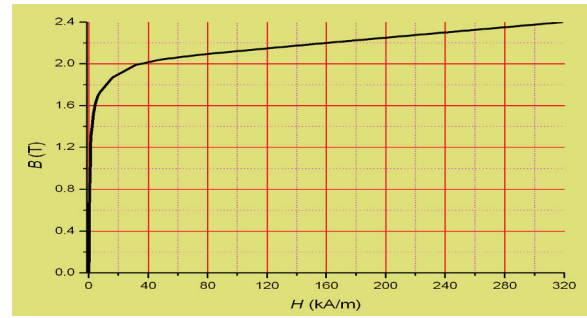


Fig. 3. The B-H curve of rotor and stator core material

The analytic results have been calculated from the equalities given according to the linear operation conditions. The relative permeability is assumed as fixed. The saturation, leakage flux and fringing effects have been ignored.

Inductance model of CFLA

As a result of the exciting the translator poles starting to overlap with the stator poles, force is generated by the inclination of the magnetic flux axis of the translator and the magnetic flux axis of the stator to align in the same direction. When the phase of the translator is in the same line with the overlapping of the stator, the translator moves pole length (l_p) with and if the excitation continues the translator remains at the brake position magnetically. If the excitation of the phase which is in the same direction at this point is interrupted and the other phases are switched respectively, the movement continues. Fig. 4 shows the translator and stator position for a part of the actuator. Here the positions are given for phase A shown by the axis line.

There are 4 coils for each phase. Fully un-aligned position is the minimum inductance position [1, 2, 7].

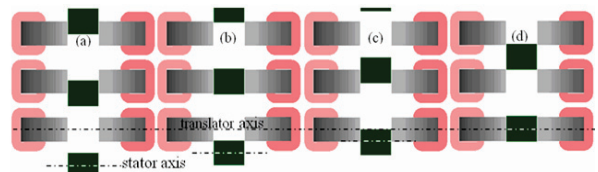


Fig. 4. Stator and translator positions a – fully unaligned; b – overlap; c – mid-aligned; d – fully aligned

Overlap position is the position where aligning starts. At the position, the phase is excited and movement starts to be aligned and inductance rises. In the mid-aligned position the inclination of to be aligned with the stator poles and the movement continue and the inductance increase. The fully aligned position is the maximum inductance position. Here the magnetic axis of the translator and stator poles are in the same direction. If the excitation continues actuator makes breaking. At this position, excitation is switched off and the other phase where the overlapping starts is switched on.

Translator has 6 poles. There are 2 double sided translator poles for each phase. The Fig. 5 shows the current direction, magnetic flux path and the magnetic circuit. Table 2 gives the magnetic circuit parameters.

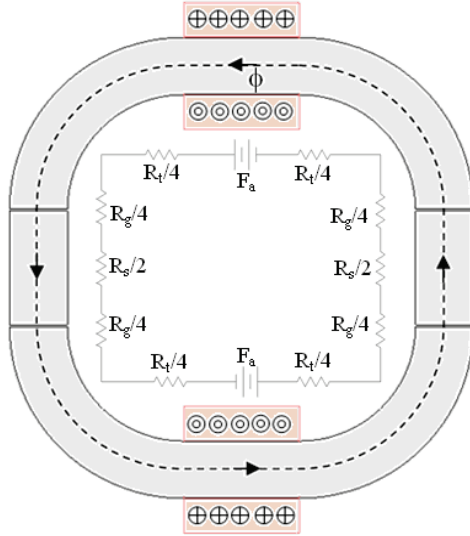


Fig. 5. Actuator core flux path and magnetic circuit

Table 2. Magnetic circuit parameters

Symbol	Explanations	Unit
R_t	Reluctance of translator	H^{-1}
R_s	Reluctance of stator	H^{-1}
R_g	Reluctance of airgap	H^{-1}
F_a	mmf for each phase	At
ϕ	Magnetic flux	Wb
l_{ft}	Length of translator flux path	m
l_{fs}	Length of stator flux path	m
l_g	Length of air gap	m
A_{ft}	Cross section of translator flux path	m^2
A_{fs}	Cross section of stator flux path	m^2
A_{fg}	Cross section of airgap flux path	m^2
N	Number of winding turns	
μ_t	Relative permeability	H/m

The actuator reluctances are divided into three: translator, stator and air gap reluctance. Their sum gives the total reluctance. The calculations will be made for the fully aligned and fully unaligned positions of the actuator. Among the reluctance parameters, the translator flux path length (l_{ft}) is calculated by (1), stator flux path length, (l_{fs}) by (2) and air gap flux path length (l_g) by (3), translator flux path cross section (A_{ft}) by (4), stator flux path cross section by (5).

$$l_{ft} = 2 \left[\pi \left(r_t - \frac{w_s}{2} \right) + w_c \right], \quad (1)$$

$$l_{fs} = 2h_{sp}, \quad (2)$$

$$l_g = 4h_g, \quad (3)$$

$$A_{ft} = w_s l_{tp}, \quad (4)$$

$$A_{fs} = w_s l_{sp}. \quad (5)$$

In order to have not zero force point in the overlap position, the length of the stator pole in the movement axis is kept 2 mm longer than the translator length. This makes the flux path cross section of the stator bigger than the flux path cross section of the translator. Therefore the flux path cross section of the air gap (A_{fg}) is given in (6) as the average of two cross sections and the total reluctance is given in (7)

$$A_{fg} = (A_{ft} + A_{fs}) / 2, \quad (6)$$

$$\Sigma R = R_t + R_g + R_s = \frac{l_{ft}}{A_{ft} \mu_r \mu_0} + \frac{l_{fs}}{A_{fs} \mu_r \mu_0} + \frac{l_g}{A_{fg} \mu_0}. \quad (7)$$

From here, the minimum inductance (L_u) for the fully un-aligned position and maximum inductance (L_a) for the fully aligned position will be calculated by the (8). The distance between these two positions is 45 mm and the inductances (L) within this range will be estimated with (9) [1, 2, 7].

$$L(x) = \frac{N^2}{R(x)}, \quad (8)$$

$$L(x, i) = [(a_0 - a_1 \cos(n_{sp} k))]. \quad (9)$$

Here x shows the position in mm which the translator takes along its movement axis. n_{sp} is the stator pole number. k coefficient is necessary to convert the linear length into angular value in the trigonometric expression and is given in (10) [6]

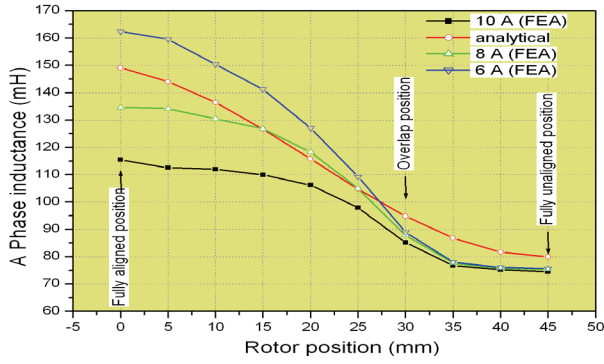
$$k = \frac{2\pi}{l_t} l_{sp}. \quad (10)$$

The coefficients a_0 and a_1 can be obtained from (11) [6–8].

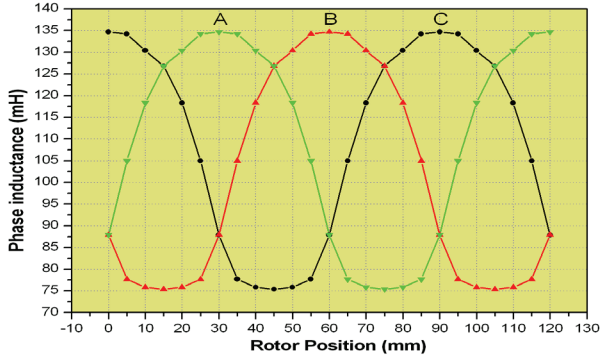
$$a_0 = \frac{1}{2}(L_a + L_u), \quad a_1 = \frac{1}{2}(L_a - L_u), \quad (11)$$

here L_a – the inductance in the fully aligned position and the maximum inductance value; L_u – the inductance in the fully unaligned position and the minimum inductance value.

Fig. 6 (a) gives the simulation and analytic inductance results of the phase a simulated between the fully unaligned and fully aligned positions. Fig. 6 (b) shows the 3 phase inductance profile for the 8 A excitation current of the actuator [7, 8].



a)



b)

Fig. 6. Inductance of the actuator: a – one phase; b – three phases

Here 10A phase current starts the actuator in the saturated region, 8A in the beginning of the saturation and 6 A in the unsaturated region. Because of the BH characteristics of the core material, the phase inductance is reduced in the saturated region.

The knee point is about 1,7 Tesla. The flux linkage (ϕ) between the fully aligned and fully unaligned positions of the actuator is obtained with the (12). Here, I is phase current. The graphics of these values is given in Fig. 7 [6–8]

$$\phi(x, i) = L(x, i) \cdot I = [(a_0 - a_1 \cos(n_{sp} k))] I \quad (12)$$

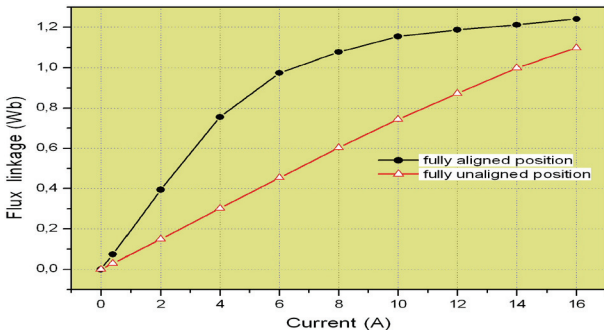


Fig. 7. Flux linkage profile of the actuator

The impact of relative permeability on inductance

In the analytic approach, the saturation effects are not taken into consideration and relative permeability is taken as fixed since the material is regarded linear in the analytical approach. When we take the relative permeability as variant between 100 - 5000, the self

inductance of a phase only in accordance with the fully aligned position is calculated and given in Fig. 8.

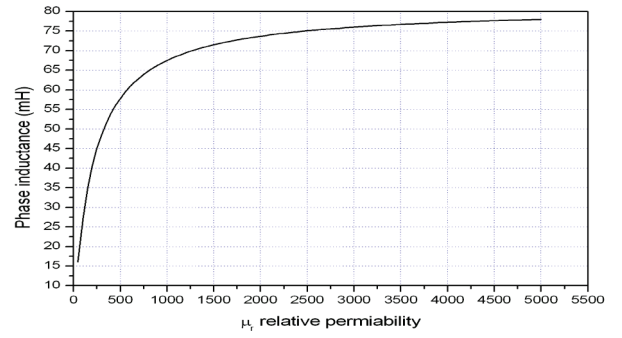


Fig. 8. The impact of relative permeability on inductance

Mutual inductances are not included in the calculation. Relative permeability takes different values in accordance with the geometry of the core in the simulation results and actual work.

The reference lines placed in the center and corner of the quadrangular and circular translator core are shown as amplitude and vectoral, and the flux density in the core is shown in Fig. 9 (a) and (b). The B values obtained from the reference lines are given graphically in Fig. 10 (a) and (b). The fact that B is variable affects the relative permeability [7, 8].

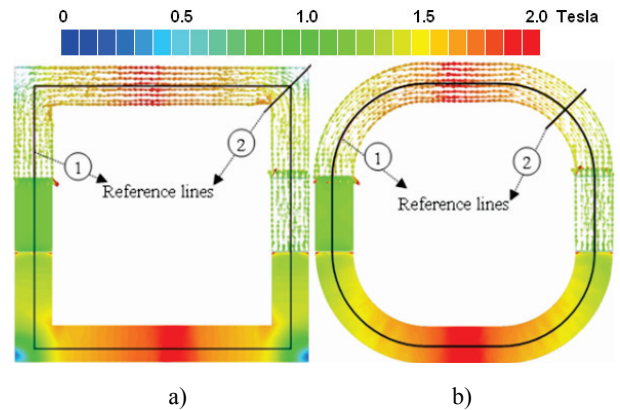


Fig. 9. Reference lines and magnetic flux distribution a- quadrangular core b- circular core

According to the values obtained from the 1st reference line placed in the center of the quadrangular core, it is observed that in the points where the flux passes the corner the flux path cross section is narrowed down and the flux values decrease from 1,5 T to 1,1 T and increase again after passing the corner. In accordance with the values obtained from the 2nd reference line placed in the corner of the core, it is observed that the flux in the quadrangular core decrease from the internal corner to the external corner and in the circular design it is observed that it passes equally from each point.

Circular flux path design is anticipated and quadrangular geometrical structure is avoided in order for the magnetic flux to be distributed uniformly and the relative permeability to be distributed in balance in every part of the core. In the corners where the flux changes direction there are impacts to reduce inductance like

leakage flux, saturation effect in the internal corners of the core and that the flux cannot use whole of the core cross section. All effects are reduced with the translator design with circular flux path.

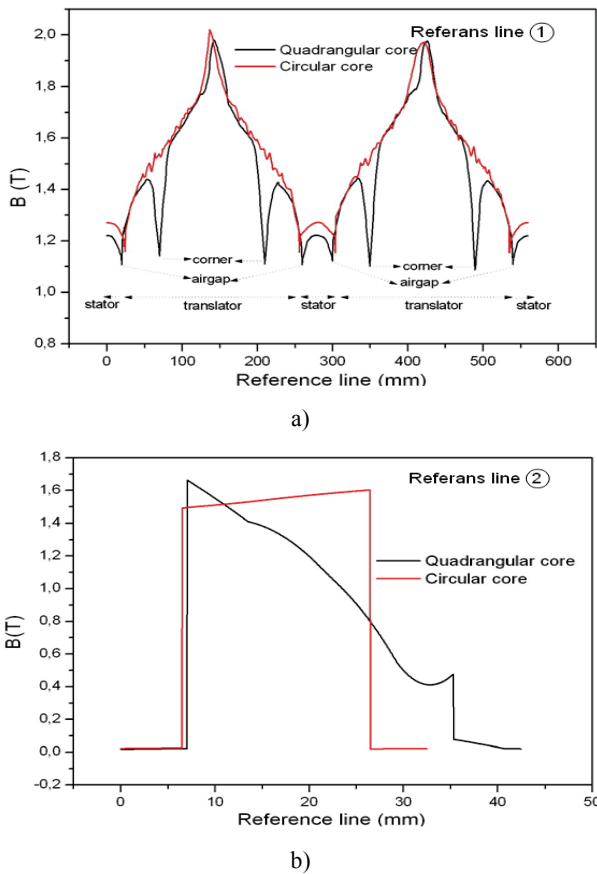


Fig. 10. Magnetic flux density in the reference lines: a – 1st reference line; b – 2nd reference line

In the excitation of the actuator phase with 10A, the magnetic flux density in the fully aligned position is given in Fig. 11 (a) as vectoral. Here it is seen that the flux direction is ok vectorally but varies in amplitude.

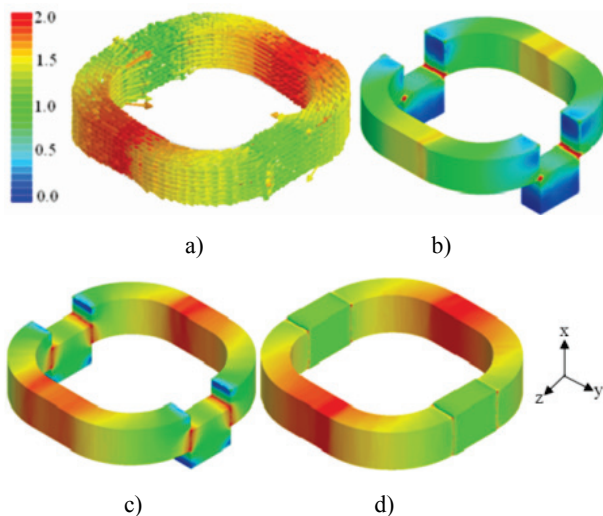


Fig. 11. a – Vectoral distribution of B in fully aligned position, amplitude distribution of B ; b – overlap; c – mid-aligned; d – fully aligned positions

Fig. 11 (b), (c) and (d) show the magnetic flux distribution of the actuator in amplitude in the overlap, mid-aligned and fully aligned positions.

In the overlap and mid-aligned positions, there is saturation in the region where the translator and stator poles overlap.

The power of the actuator varies depending on the inductance and position. The W_c co-energy taking place in a phase of the actuator is given in (13) in joule

$$W_c = \frac{1}{2} \frac{dL(x,i)}{dx} \quad (13)$$

The force in the movement axis (x) of the actuator is called propulsion force. Magnetic flux path is perpendicular to the (y) in the region it passes through the stator. No force is generated in this axis as the flux path of the translator and stator is aligned with the (y) axis. The force with which the stator and translator pulls each other is the one which is formed in the (z) axis.

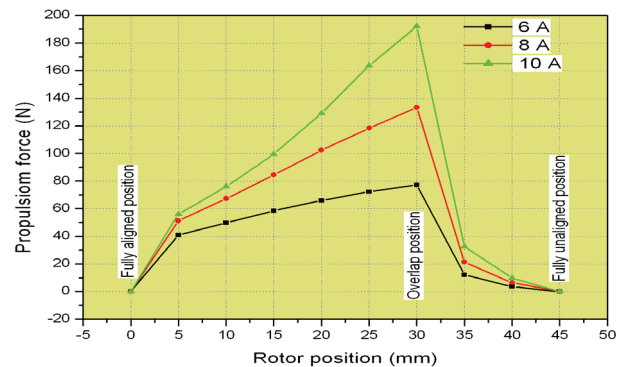


Fig. 12. Force profile of the actuator

However, they eliminate each other as their alignment and amplitude are the same but the direction is different. The total force in the (z) axis is zero. The propulsion of the actuator is given in Fig. 12 in accordance with the results of the finite elements analysis.

Conclusion

In this study, the circular structure of the translator will ensure uniform distribution of the magnetic fluxes and reduce the change of the relative permeability. 2 independent flux paths take place with one phase excitation in the double sided design and 2 coils and 4 air gaps on each flux path ensure high force with low phase inductance. Double sided translators provide mutual movement and generate high propulsion in the movement axis and compensating forces in other axes. Coils have been placed on mobile and double sided translators to allow less coil and core material. Thus a low-cost and light mobility have been obtained for long distance linear movement systems. Stator and translators parts have been placed yokelessly and independently from each other. This provides a light and low cost stator. As the translator parts are independent from each other, maintenance and repairing will be easily by removing only the defective part. Besides, because the stator parts are independent from each other, the length of the linear movement system can

be extended as desired by adding new parts without disrupting the design [6]. This system is offered as an advantageous design for the horizontal transportation system.

References

1. **Krishnan R.** Switched Reluctance Motor Drives // Washington D. C.: CRC Press, 2001. – P. 17–23.
2. **Kang D. H., Jeong, Y. H., Kim, M. H.** A Study on the Design of Transverse Flux Linear Motor with High Power Density // Proceeding ISIE 2001. – Busan, Korea, 2001. – P. 707–711.
3. **Lim H. S., Krishnan R., Lobo N. S.** Design and Control of a Linear Propulsion System for an Elevator Using Linear Switched Reluctance Motor Drives // IEEE Transactions On Industrial Electronics, 2008. – No. 55(2). – P. 1584–1591.
4. **Lim H. S., Krishnan R.** Ropeless Elevator With Linear Switched Reluctance Motor Drive Actuation Systems // IEEE Trans. On Ind. Electronics, 2007. – No. (4)54. – P. 2209–2218.
5. **Daldaban F., Ustkoyuncu N.** A new double sided linear switched reluctance motor with low cost // Energy Conversion and Management, 2006. – No. 47. – P. 2983–2990.
6. **Fenercioğlu A., Dursun M.** Design And Magnetic Analysis of A Double Sided Linear Switched Reluctance Motor // 14th ISEF 2009. – Arras, France, 2009. – P. 473–474.
7. **Gürdal O., Fenercioğlu A.** Helisel Yapılı Anahtarlamalı Relüktans Motorun Bilgisayar Destekli 3 Boyutlu Manyeto statik Analizi, (HS–SRM) // Journal of Engineering Faculty Gazi University, 2007. – No. 2(22). – P. 315–322.
8. **Fenercioglu A., Tarimer İ.** Anahtarlamalı Relüktans Motorlarda Faz Endüktansına Etki Eden Faktörlerin İncelenmesi // Pamukkale University Journal of Engineering Science 2007. – No. (2)13. – P. 145–150.

Received 2010 02 18

A. Fenercioğlu. Design and Magnetically Analysis of Circular Flux Linear Actuator // Electronics and Electrical Engineering. – Kaunas: Technologija, 2010. – No. 5(101). – P. 21–26.

In this study design of the circular flux linear actuator (CFLA), three dimensional FEM analysis and analytical approach have been examined. The actuator designed has active translator and passive stator. The number of phase is 3 and there are 6 translator poles. The movement is achieved by 4 pairs of stator poles placed between the corresponding translator poles. The circular translator poles are recommended independently from each other to ensure uniform flux distribution. The weight is lower because there is no joint core and back iron. The maintenance and repair of separate parts are facilitated. Design has been planned as double sided to compensate the forces in the axes other than the movement axis. This provides high force at low inductance with two coils and 4 air gaps in each phase. Stator parts consist of independent double poles. Movement distance can be extended by attaching these poles along the movement axis. The inductance and force parameters of the modeled CFLA have been obtained by simulation works. III. 12, bibl. 8, tabl. 2 (in English; abstracts in English, Russian and Lithuanian).

A. Фенерциоглю. Исследование магнитных свойств кольцевого линейного привода // Электроника и электротехника. – Каунас: Технология, 2010. – № 5(101). – С. 21–26.

Описывается новый вариант кольцевого линейного привода, работающего в трехмерной координатной системе. Органичность прибора заключается в том, что имеет пассивный шестиполосный ротор и работает от трехфазной сети. Установлено, что для уменьшения разброса магнитного потока кольцевые полюса целесообразно рассматривать как отдельные элементы. Таким образом уменьшается вес прибора и увеличивается расстояние движения прибора. Расчет параметров привода осуществляет методом моделирования. Теоретические результаты достаточно хорошо соответствуют экспериментальным. Ил. 12, библи. 8, табл. 2 (на английском языке; рефераты на английском, русском и литовском яз.).

A. Fenercioğlu. Tiesiaeigės žiedinės pavaros projektavimas ir magnetinių savybių analizė // Elektronika ir elektrotechnika. – Kaunas: Technologija, 2010. – Nr. 5(101). – P. 21–26.

Suprojektuota žiedinė tiesiaeigė pavara. Atlikta analizė taikant baigtinių elementų metodą trimatėje koordinačių sistemoje. Suprojektuota trifazė šešiapolė pavara turi aktyvųjį transliatorių ir pasyvųjį rotorių. Judesiui atlikti panaudotos keturios statoriaus poliaus poros, išdėstytos tarp atitinkamų transliatorių polių. Dėl tolygaus magnetinio srauto pasiskirstymo rekomenduojama žiedinius transliatoriaus polius montuoti kaip atskirus elementus. Tokios pavaros svoris yra mažesnis, nes nėra bendros jungiamosios šerdies. Statorius susideda iš dviejų nepriklausomų polių. Pridėjus šiuos polius išilgai judėjimo krypties gali būti pailgintas pavaros judėjimo atstumas. Atliktas induktyvumo ir jėgos parametrų modeliavimas. Il. 12, bibl. 8, lent. 2 (anglų kalba; santraukos anglų, rusų ir lietuvių k.).